

# Study of Gas Turbulent Dispersion Process in the Alcântara Launch Center

Adrián Wittwer<sup>1</sup>, Acir Loredou-Souza<sup>2</sup>, Mario Oliveira<sup>2</sup>, Gilberto Fisch<sup>3</sup>, Bianca de Souza<sup>4</sup>, Elisa Goulart<sup>5</sup>

Wittwer A  <https://orcid.org/0000-0001-9716-4375>  
Loredou-Souza A  <https://orcid.org/0000-0002-6648-8315>  
Oliveira M  <https://orcid.org/0000-0001-8014-9160>  
Fisch G  <https://orcid.org/0000-0001-6668-9988>  
Souza B  <http://orcid.org/0000-0002-9775-6378>  
Goulart E  <http://orcid.org/0000-0002-0051-0778>

## How to cite

Wittwer A; Loredou-Souza A; Oliveira M; Fisch G; Souza B; Goulart E (2018) Study of Gas Turbulent Dispersion Process in the Alcântara Launch Center. J Aerosp Technol Manag, 10: e4318. doi: 10.5028/jatm.v10.956.

**ABSTRACT:** The Alcântara Launch Center (ALC) is the Brazilian gate to the space located at the north coast of Maranhão State, close to the Equator. Topographical local characteristics modify the parameters of incident atmospheric winds and it can cause great influence on the gas dispersion process. In this work, detailed scale models of the ALC region was experimentally evaluated using a wind tunnel. The topographical scale models were built where mean and fluctuating flow characteristics were analysed in order to understand the real behaviour of ALC winds and then, simulations of the effluent dispersion process were made using these scale models. The wind velocity was measured by a hot wire anemometer and the concentration fields in the proximities of a gas emission source were analysed by an aspirating probe connected to the anemometer system. The results obtained show similarity with numerical outputs from previous study in the case of the emission at ground level. A coherent behaviour with the physic of the phenomena was observed for the case of emission downward.

**KEYWORDS:** Wind tunnel, Gas concentration, Diffusion, Aspirating probe.

## INTRODUCTION

It is possible to study and investigate the physical and dynamics phenomena that occur in the planetary boundary layer by experimental studies, like using wind tunnels (WT), and their results can be used to validate theoretical and numerical models. The high costs of *in situ* experiments have led to a higher use of WT with small scale models, such as in the studies of atmospheric pollutant dispersion and characterization of atmospheric winds.

In the literature, many studies involving the application of WT can be cited: physical simulations considering the forest and atmosphere coupling in the analysis of turbulent structures of the atmosphere (Novak *et al.* 2000), dispersion experiments of pollutants immersed in obstacles (Marvoidis *et al.* 2003), and flow simulation of complex topographies as in the works of Cao and Tamura (2006) and Faria (2016).

1.Universidad Nacional del Nordeste – Facultad de Ingeniería – Resistencia/Chaco –Argentina.

2.Universidade do Rio Grande do Sul – Laboratório de Aerodinâmica das Construções – Porto Alegre/RS – Brazil.

3.Departamento de Ciência e Tecnologia Aeroespacial – Instituto de Aeronáutica e Espaço – Divisão de Ciências Atmosféricas – São José dos Campos/SP – Brazil.

4.Universidade Federal do Espírito Santo – Departamento de Engenharia Mecânica – Vitória/ES – Brazil.

5.Universidade Federal do Espírito Santo – Departamento de Engenharia Ambiental – Vitória/ES – Brazil.

**Correspondence author:** Bianca de Souza | Universidade Federal do Espírito Santo – Departamento de Engenharia Mecânica | Av. Fernando Ferrari, 514 | CEP: 29.075-910 – Vitória/ES – Brazil | E-mail: biancahulle@gmail.com

Received: Mar. 13, 2017 | Accepted: Nov. 29, 2017

**Section Editor:** Rosa Marques



The characterization of the atmospheric flow in the main Brazilian rocket launching base, the Alcântara Launch Center (ALC), is of great importance in the design and construction of rockets, in the calculations of its trajectory as well as the control and guidance system (Roballo and Fisch 2008). The atmospheric flow of this region presents particular characteristics and it is a product of ocean-continent circulation interactions.

In addition, the study of dispersion processes of pollutants on the ALC region is of great importance in environmental matters like local flora and fauna and the quality of human life in the vicinity of the launch center. It should be taken into consideration that features such as pollutant (or any other study subject) concentration and its value fluctuation in an area near the emission site are not determined only by its geographical configuration, but also by the physics of the flow itself such as atmospheric wind turbulence (Wittwer *et al.* 2016a). To do so, experimental techniques of conditioned sampling are used to analyze the intermittent processes of large bursts of wind and velocity values near zero, as expected in Gaussian processes (Jensen and Busch, 1982). Complementing, Wittwer *et al.* (2007a) found that in case of intermittence, extreme values may be more critical than average values, thus, to characterize it, it would be necessary to analyze the probability distributions and measure their fluctuations.

Regarding the studies of the dispersion processes in the WT itself, it is important to consider additional information, such as visualization tests and quantitative tests of concentration measurement in areas of interest as reported by Kastner-Klein and Plate (1999). In experiments to measure concentration in turbulent dispersion processes, an important variable is the type of tracer gas used to simulate the emission (Wittwer *et al.* 2016a). Measurement of concentration fluctuations can be performed by a hot anemometer using an aspirating probe (Harion *et al.* 1995), as described in details by Wittwer (2006).

Numerical simulations of turbulent diffusion process were also developed by different authors (Delaunay *et al.* 1997; Meroney *et al.* 1999). Eulerian models are more adapted for pollutant dispersion on complex topography (Zanetti 1990). Turbulence parameterization for boundary layer is a critical aspect in numerical dispersion modelling (Degrazia *et al.* 2000). Recently, Schuch and Fisch (2017) presented a numerical study of the dispersion for ALC using the meteorological model WRF coupled with its chemistry module (CHEM).

In the present study, experiments were performed in WT Prof. Joaquim Blessmann (Blessmann 1982) to analyze the turbulence dispersion process at the ALC region. For the essays, the topography of the region of interest was constructed on a reduced scale of 1/400. The velocity profiles and wind speed fluctuations, obtained by hot wire anemometer techniques, were analysed at various points in the model. Mean concentration and intensity of concentration fluctuation profiles were measured and different emission conditions were compared.

---

## LOCALIZATION AND CHARACTERISTICS OF THE ALCÂNTARA LAUNCH CENTER

The Alcântara Launch Center is located on the north coast of the state of Maranhão, Brazil (Fig. 1), at the geographic coordinates 2°19' S, 44°22' W, 50 msl and at a distance of 30 km from the city of São Luiz, Maranhão. Figure 2 shows the respective localization of the ALC, the Mobile Tower Integration (MTI) where rockets are launched, and the Anemometric Tower (AT) where data are collected to analyze the surface wind profile characteristics. This place is close to the sea and the vegetation is characteristic of restinga, with trees ranging from 2.0 up to 3.0 m height.

The wind regime is very distinct between both seasons but the wind direction is predominantly from east, reaching maximum velocities between 10.0 and 15.0 m/s at 2000 m height. The sea breeze is more intense during the dry period due to the thermal difference between oceanic and continental surface. For strong winds, wind speed higher than 10.0 m/s, the flow is sufficient turbulent to mix vertically the atmosphere and suppress the thermal effects (Loredou-Souza *et al.* 2004). Consequently, for this near neutral conditions, the atmospheric turbulence is purely originated from the wind shear (mechanically driven) and depends of the friction of the surface and the vertical wind shear. This work assumes a neutral stability at ALC due to the strong winds. A complementary study using a different data-set made with sonic anemometer measurements (Magnago *et al.* 2008) confirmed this hypothesis.

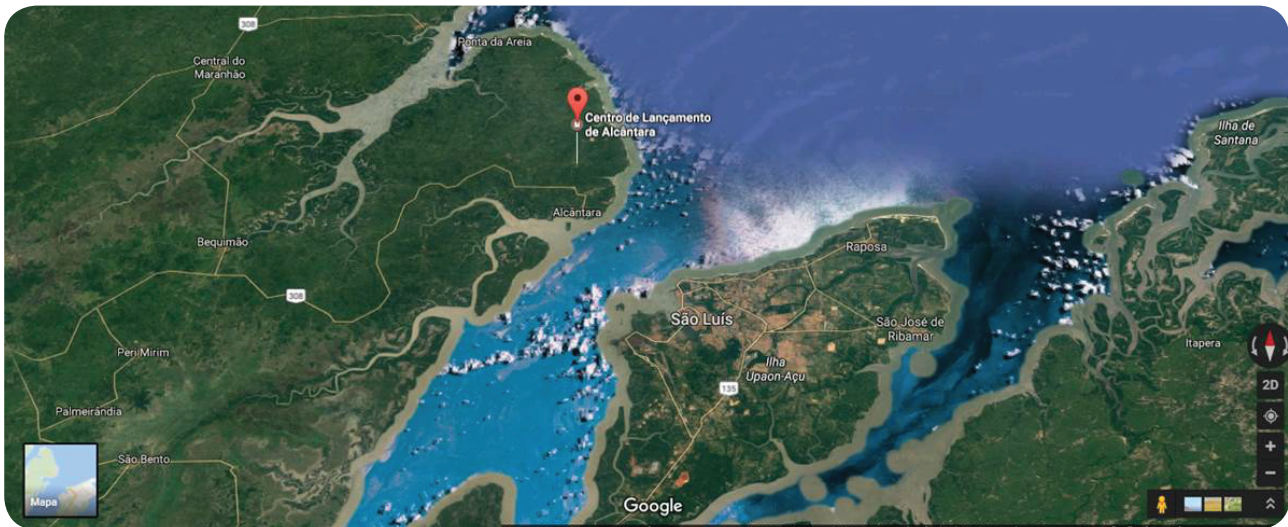


**Figure 1.** Spatial location of the Alcântara Launch Center obtained through satellite image using Google Earth on 07/02/2017 at 9:00 p.m.

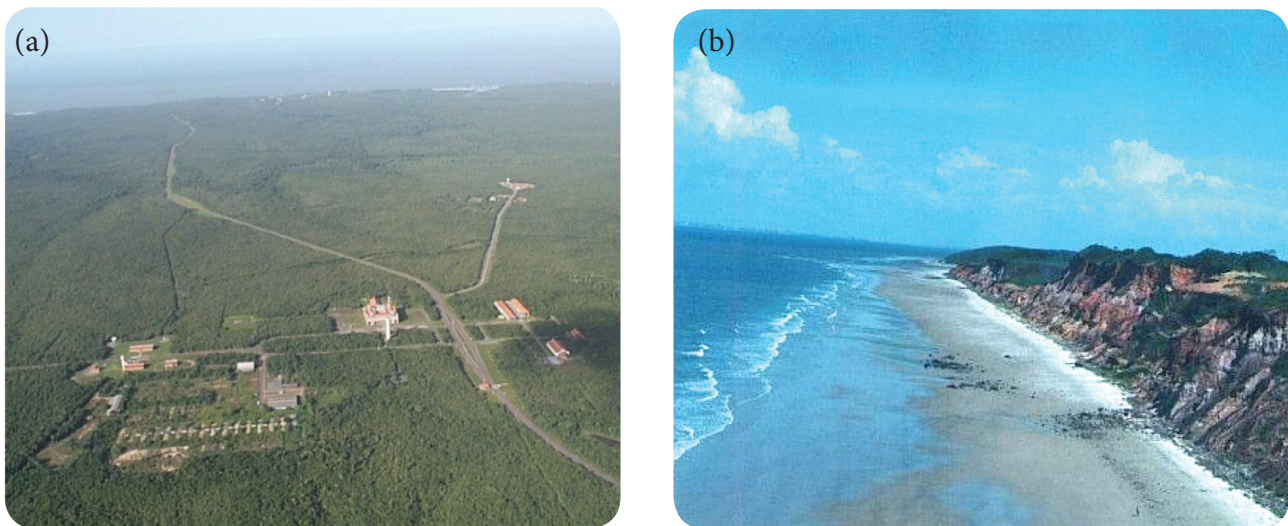


**Figure 2.** (a) Localization; and (b) topographic characteristics of the Alcântara Launch Center (Pires *et al.* 2015).

## EXPERIMENTAL ARRANGEMENTS

### CHARACTERISTICS OF THE “PROF. JOAQUIM BLESSMANN” WIND TUNNEL

The tests were performed in the Wind Tunnel (WT) Prof. Joaquim Blessmann. Briefly, it is an enclosed return boundary wind tunnel, specifically designed for static and dynamic testing of civil engineering construction models. The correct simulation of the main characteristics of natural wind in wind tunnels is a basic requirement for applications in Civil Engineering, without which the results obtained can deviate considerably from reality.

Pioneer in Latin America, the WT Prof. Joaquim Blessmann, from the Federal University of Rio Grande do Sul, Porto Alegre, Brazil (Blessmann 1982), has a length/height ratio of the test chamber greater than 10. The velocity of the airflow in this chamber, uniform flow without any models, exceeds 46 m/s. The equipment allows the simulation of the main characteristics of natural winds in the atmospheric boundary layer and allows the correct determination of the working pressures on the facades and structure of the buildings.

## INCIDENT WIND SIMULATION

In Wind Engineering, the vertical variation of the mean velocity  $U$  is usually expressed from the potential law, which is valid throughout the boundary layer. This law is defined by Eq. 1, where  $U_{ref}$  is the reference velocity obtained at the reference height  $z_{ref}$  (usually assumed as 10 m). The exponent  $\alpha$  varies from 0.09 to 0.45, depending on the surface roughness of the terrain and the thermal stability. Atmospheric turbulence is characterized by the turbulence intensity  $I_u$ , defined by the ratio between the standard deviation of the fluctuations  $u'$  and the mean velocity  $U$ . Complementarily, the turbulence spectrum allows to evaluate the energy distribution as a function of frequency. Measurements made in the atmosphere allow evaluation of the atmospheric spectra, which are then used to validate the results obtained in wind tunnels.

$$U/U_{ref} = (z/z_{ref})^\alpha \quad (1)$$

In order to study the aerodynamic phenomena that occur in the atmospheric boundary layer, it is necessary to simulate inside a WT. The simulation process consists of developing a physical model of the atmospheric flow so the characteristic parameters are reproduced in the best possible way inside the tunnel. In most laboratories it is more common to simulate the neutral boundary layer. This implies modeling the distribution of mean velocities, turbulence scales and atmospheric power spectrum (Surry 1982). Counihan (1969) and Standen (1972) employing roughness methods, barrier and blending devices, have developed particularly suitable simulation techniques for reproducing boundary layers under conditions of neutral stability. These techniques allow us to obtain representations of the boundary layers that occur on rural and urban lands. In a previous work, Loredou-Souza *et al.* (2004) carried out a detailed description of the systems, methodologies and ways of evaluating the physical models of atmospheric flow in a neutrally stable in boundary layer wind tunnels.

According to the characteristics of the roughness of the terrain around the ALC, a wind profile was simulated using a potential profile of mean velocities and exponent  $\alpha = 0.11$  (representative roughness of Category I) according to NBR 6123 (Blessmann 1995). The roughness characteristics of the simulated terrains correspond to a large smooth surface, more than 5 km in length, measured in the direction of the incident wind. The simulators used to simulate the wind characteristics are shown in Fig. 3.



**Figure 3.** Entrance of the wind tunnel and the turbulence generator.



Based on the characteristics of the site under study and the landscape at ALC, it was tested the model for incident winds with these characteristics. Around the model, the closest buildings were reproduced on the scale of the model so that the flow conditions corresponded as closely as possible to the real conditions. The main characteristics of the simulated winds can be seen in Fig. 4, where the vertical profile of the mean velocities  $U(z)/U(450)$  is indicated, where  $U(450)$  is the mean velocity in the longitudinal axis of the tunnel, the intensity of turbulence  $u'/U$  and the macro-scale  $Lu$  of the longitudinal component of the turbulence.

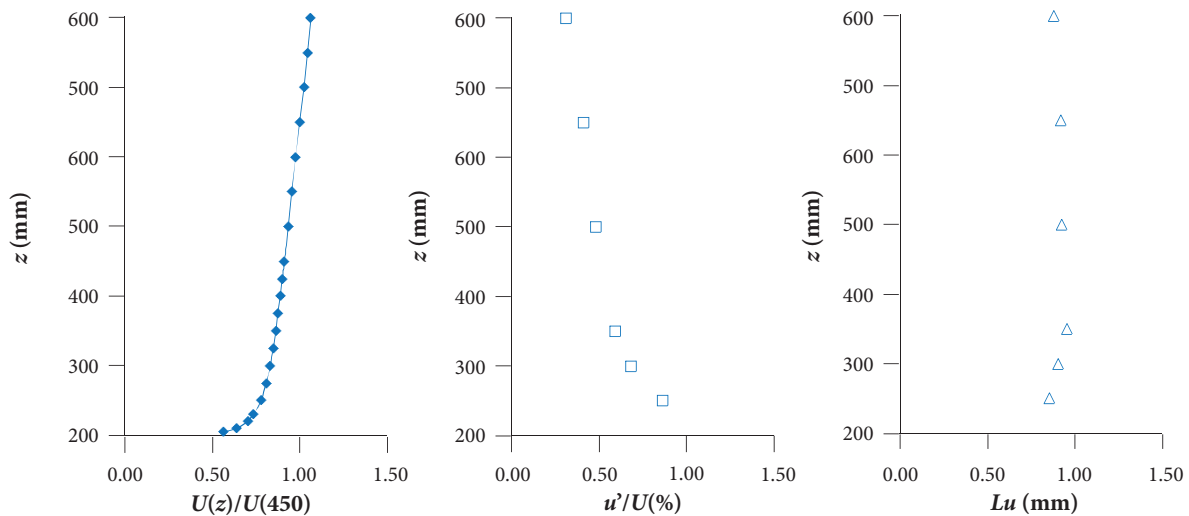


**Figure 4.** Main characteristics of the incident flow [exponent  $\alpha = 0.11$ ].

## CONCENTRATION MEASUREMENTS

The study of dispersion processes based on wind tunnel experiments requires measuring the concentration of a given gas. The measurement system depends on the type of gas used as a tracer and for this work a hot wire anemometer was used combined with an aspirating probe (Wittwer 2006). From the calibration process, the suction probe allows direct determination of instantaneous concentration values for a binary mixture. The gas flows and concentration of the binary mixtures were necessary to correctly simulate the problems and phenomena of dispersion in the wind tunnel, and also to calibrate the instruments of measurement of the concentrations.

To obtain binary mixtures of gases with fixed velocity and flow, it was used the device shown in Fig. 5a. This device was built in the Aerodynamics Laboratory of the Buildings of Universidade Federal do Rio Grande do Sul (UFRGS). The mixture was obtained by two series of small holes of different diameters that work as sonic tubes. Each of the series of holes allows an accurate flow of helium and air, respectively, and with the interconnection at the end of the circuit the exact mixture is obtained. The degree of accuracy of the mixing device depends on the number of sonic tubes and the accuracy with which the orifices are calibrated. The relative errors are larger in the smaller diameter holes, in this case 0.50 mm. The mass concentration ( $C$ ) corresponds to a mixture of helium (He) and air flows, and it is evaluated by Eq. 2.

$$C = \frac{Q_m(\text{He})}{Q_m(\text{He}) + Q_m(\text{Ar})} \quad (2)$$

In order to use the hot wire anemometer in the measurement of gas concentrations it is necessary to construct a probe in which the hot wire is sensitive to variations in gas density and insensitive to variations in the velocity of the outside flow. Therefore an aspirating probe consisting of the hot wire of the anemometer and an external tube (Fig. 5b) was used, which was connected to a vacuum pump and allows to measure the instantaneous fluctuations of density or concentration. The capillary tube, together with

the aspiration, causes the sonic blockage. The hot wire thus becomes a sensor that notices the variations of the thermal properties of the fluid in the process of heat transfer, that is, it measures the variations of gas concentration.

The dynamic response of the aspirating probe can be analysed by constructing concentration spectra. Results obtained for a helium-air coaxial jet using different frequencies of acquisition between 5 and 10 kHz guarantee the dynamic response of this type of probe to frequencies above 1 kHz. The characteristic scales in wind tunnels usually do not require the analysis of frequencies greater than 1 kHz (Loredo-Souza and Wittwer 2010).

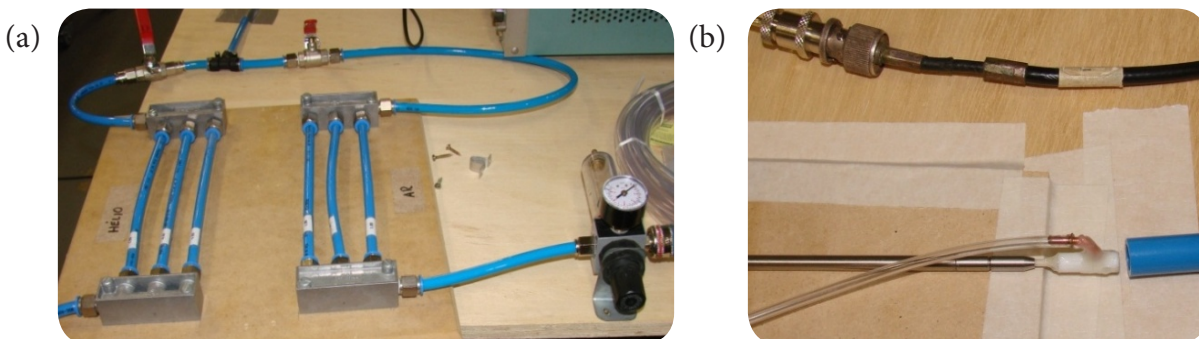


**Figure 5.** (a) Calibration system; and (b) aspirating probe.

## EVALUATION OF THE ALCANTARA LAUNCH CENTER ATMOSPHERIC FLOW

The analysis of the atmospheric flow was based on two important physical characteristics: velocity profiles and fluctuations at different points of interest in the studied region. Figure 6 shows representative models of the three angles of wind incidence analysed, nominally  $0^\circ$ ,  $30^\circ$  and  $330^\circ$ . The choice of incidence angles was based on wind directions with  $\pm 30^\circ$  variability, predominantly, from the marine coast of the ALC region (Gisler *et al.* 2011).

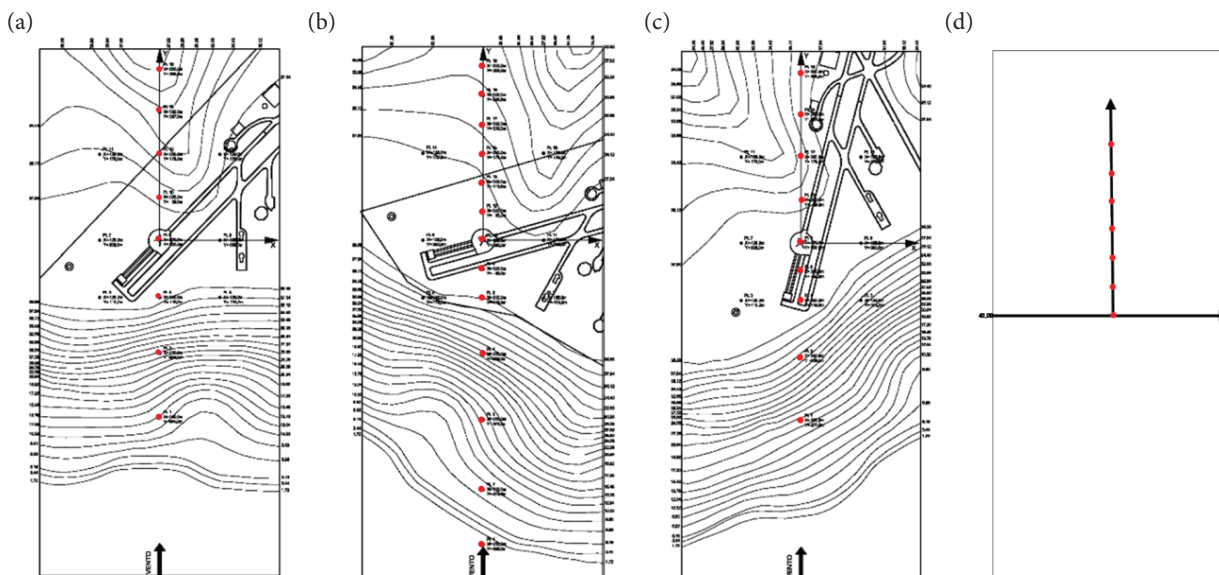


**Figure 6.** Models built on reduced scale (1/400) of ALC for the three directions of wind incidence: (a)  $0^\circ$ , (b)  $30^\circ$  and (c)  $330^\circ$ , and (d) the simplified model (Step-like).

This initial evaluation consisted of studying the atmospheric flow characteristics and gas dispersion processes in the ALC region. The results of the evaluation of the flow in the vicinity of the ALC are presented in a complementary work (Wittwer *et al.* 2016b) where a quantitative analysis of vertical profiles of mean velocity and turbulence intensity was carried out. In addition, the results were compared with the type of topographic model used in the study for the three directions of wind incident in the WT. Basically, this study allows determining the points where the largest flow variations occur in the vicinity of the surface with respect to the incident flow.

Wittwer *et al.* (2016b) presented, in a complementary way, the atmospheric flow results obtained with a simplified step-like model (Fig. 6). An interesting conclusion obtained from this evaluation is that simplifications can lead to results that do not reflect the actual situation. Consequently, it is important to emphasize the importance of using topographic models that reproduce the surrounding environment by applying a defined geometric scale according to the scale of the incident wind, in order to obtain reliable results in WT studies.

A previous work was developed by Marinho Pires *et al.* (2010) where atmospheric flow measurements were carried out using the PIV and HWA techniques on a simplified wind tunnel model of the ALC region constructed with a scale factor of 1:1000. Also, full scale *in situ* wind measurements using aerovanes and sonic anemometers at Alcântara Launch Center were previously analysed by Fisch (2010). These studies were used to define the 1/400 scale model constructed for the present work and they can be used to translate the results obtained at the scale model to analyse the full-scale problem.

## EXPERIMENTAL ANALYSIS OF THE TURBULENT DISPERSION PROCESS

Basically, the topographic model studied is representative of the Alcântara Launch Center, with a 0° angle deviation for the predominant wind direction. However, a complementary measurement was made with the model corresponding to the wind incident in the direction 330°, that is, with a wind direction rotation of 30° (Fig. 7). The preliminary results of the dispersion study use a wind tunnel with reproduction of the atmospheric flow, which were simulated from the small scale models that reproduce the topographic conditions and simulate the atmospheric flow of the ALC region. The dispersion process was evaluated using a hot wire anemometer with an aspirating probe. The dimensionless concentration coefficient  $K$  is defined as Eq. 3.

$$K = \frac{CU_{ref}H^2}{Q_0} \quad (3)$$

where:  $C$  is the measured concentration;  $U_{ref}$  is the reference velocity;  $H$  is the reference height of 160 m; and  $Q_0$  is the emission flow rate. The intensity of the concentration fluctuations  $I_c$  is defined by the ratio of the standard deviation of the fluctuations  $c'$  to the maximum value of the mean concentration at the profile  $C_{ref}$  (Eq. 4).

$$I_c = \frac{c'}{C_{ref}} \quad (4)$$

The corresponding tests were carried out with average wind speeds of 2.60 m/s, although speeds of 1.65 and 4.50 m/s were used in specific cases. At the emission source, located in the launch area, was used helium gas. The emission conditions were varied to evaluate the emission thrust effect in the dispersion process. At this stage, the study was divided into two parts. In the first stage the dispersion process corresponding to a vertical emission from bottom to top, with exit at the level of the ground, at the point of the launching of the rockets (Fig. 8a) was evaluated. Next, the direction of the emission was inverted (top to bottom), trying to simulate the emission caused by a rocket (Fig. 8b).

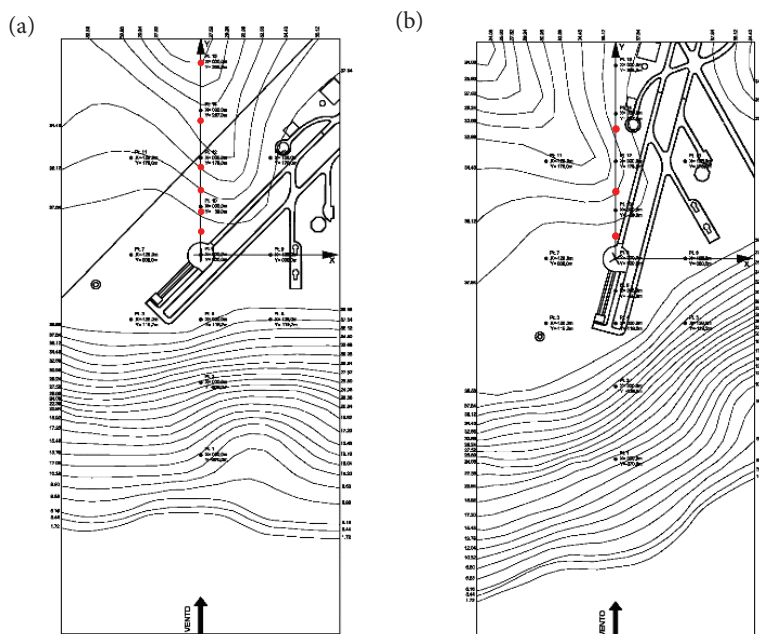
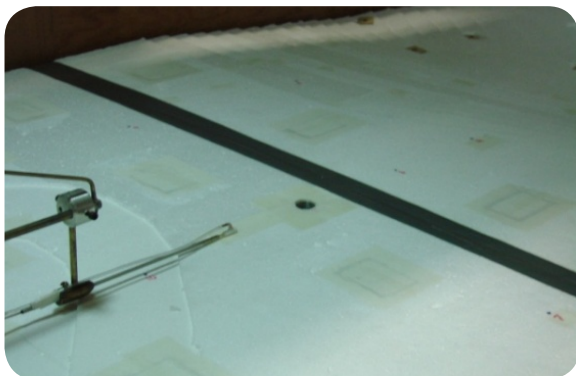


Figure 7. Topographic models developed for two incident wind directions (a) 0°; and (b) 330°.

(a)



(b)



Figure 8. (a) Emission at ground level upward; and (b) emission downward simulating the rocket (Wittwer et al. 2016a).

**RESULTS FOR EMISSION AT GROUND LEVEL - MODEL 0°**

In Table 1 are indicated the characteristics that define the conditions of dispersion of the plume for the ground level emission (A, B, C and D). The measuring locations are indicated in the graphs by the dimensionless coordinates  $(x/H, y/H)$ . Figure 9 presents the vertical profiles of the non-dimensional mean concentration  $K/K_m$  and the intensity of the concentration fluctuations  $I_c$ , obtained with emission at the ground level in the leeward positions of the emission, with spacings and  $/H$  of 0.25, 0.50, 1.00, 1.50 and 2.25, respectively, for the reference height  $H = 400$  mm. The emitted helium flow rate was  $0.176 \text{ dm}^3/\text{s}$  and the reference air velocity is  $2.60 \text{ m/s}$ , which define condition A for the emission plume as can be seen in Table 1.

Figure 10 shows the vertical profiles of concentration  $K$  and intensity  $I_c$  obtained with a helium flow rate of  $0.703 \text{ dm}^3/\text{s}$  and the same air reference velocity ( $2.60 \text{ m/s}$ ), which determine condition B for the emission pen. The leeward positions of the emission are  $y/H$  of 0.25, 0.50, 1.00, 1.50, and 2.25, respectively.

The vertical profiles of concentration  $K$  and the intensity of concentration fluctuations  $I_c$  corresponding to condition C for the emission plume, obtained with a helium flow of  $1.582 \text{ dm}^3/\text{s}$  and air velocity of  $2.60 \text{ m/s}$ , are shown in Fig 11. The locations



evaluated are  $y/H = 0.50, 1.00, 1.50$  and  $2.25$ , respectively. The condition D, defined from an emission of  $1,582 \text{ dm}^3/\text{s}$  of helium and an air reference velocity of  $1.65 \text{ m/s}$ , was analysed in Fig. 12, where the vertical profiles are shown in the leeward positions of the emission at  $H = 1.00$  and  $2.25$ .

Figure 13 presents the horizontal profiles, which allow evaluating the lateral symmetry of the emission plume with only three concentration profiles being evaluated. For condition B of the emission plume, the leeward positions of the emission were evaluated at  $H = 0.50$  and  $2.25$ . In the further leeward position, a displacement of the center of the plume is observed. For condition D, the horizontal profile at the  $y/H = 1.00$  position shows a lateral displacement of the center of the plume similar to that obtained for condition B.

**Table 1.** Conditions for emission at ground level.

Condition	$Q_0$ [ $\text{dm}^3/\text{s}$ ]	$w_0$ [ $\text{m/s}$ ]	$U_{\text{ref}}$ [ $\text{m/s}$ ]	$w_0/U_{\text{ref}}$
A	0.176	0.560	2.60	0.215
B	0.703	2.238	2.60	0.861
C	1.582	5.036	2.60	1.937
D	1.582	5.036	1.65	3.052

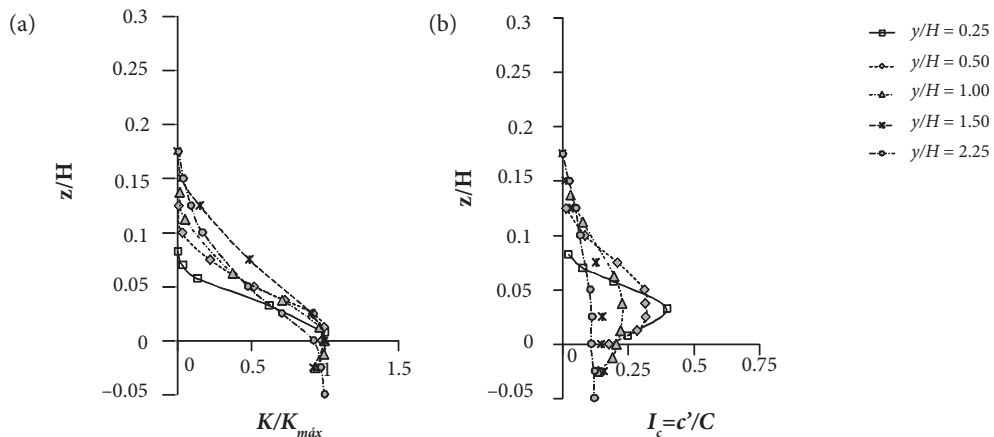


**Figure 9.** Vertical profiles of concentration (a)  $K/K_{\text{máx}}$ ; and (b)  $I_c$  for condition A.

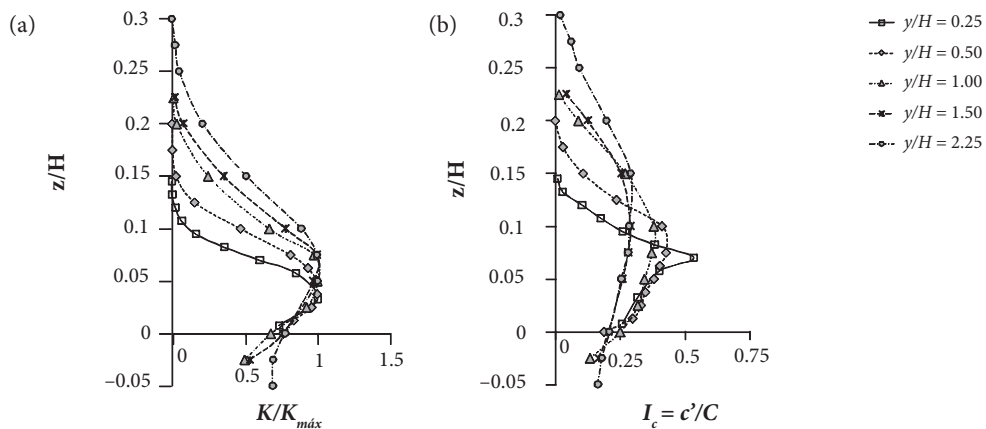


**Figure 10.** Vertical profiles of concentration (a)  $K/K_{\text{máx}}$ ; and (b)  $I_c$  for condition B.

The results are complemented with the values of  $K_{max}$  indicated in Table 2. These values allow evaluating the dispersion process evolution in terms of the leeward position related to the emission location. In general, the results show consistency with respect to the dilution of the concentration values for the different conditions analysed, as well as in the relation of the distributions of

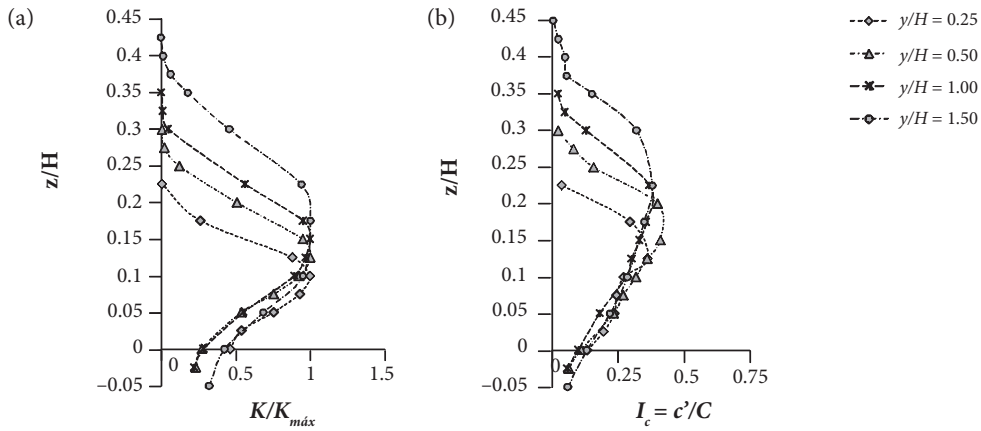


Figure 11. Vertical profiles of concentration (a)  $K/K_{max}$ ; and (b)  $I_c$  for condition C.

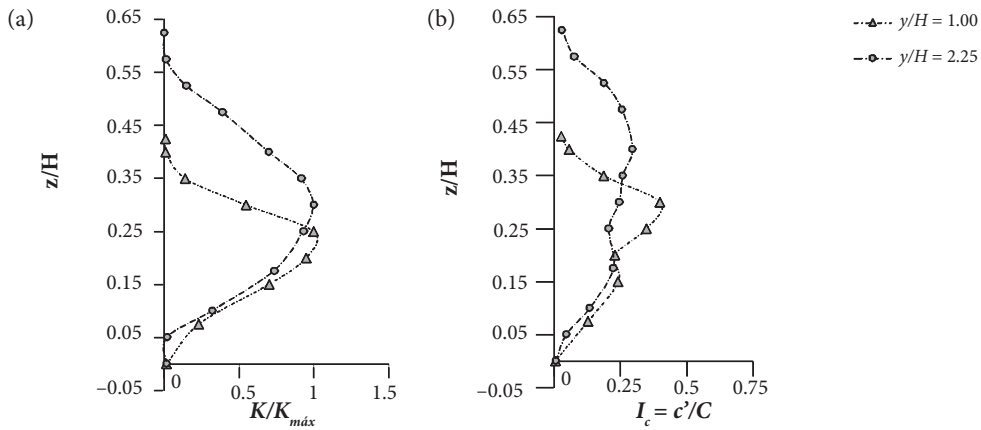


Figure 12. Vertical profiles of concentration (a)  $K/K_{max}$ ; and (b)  $I_c$  for condition D.

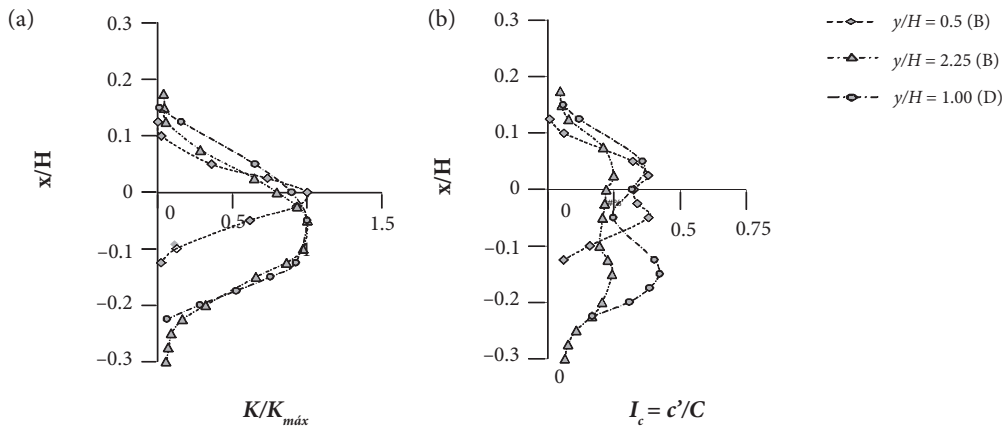


Figure 13. Horizontal profiles of concentration (a)  $K/K_{max}$ ; and (b)  $I_c$  for conditions B and D.

the measured values in the leeward positions of the emission and laterally. The measurements were made considering only the incident wind direction corresponding to  $0^\circ$  (perpendicular to the coast).

**Table 2.** Values of  $K_{max}$  for emission at ground level – model  $0^\circ$ .

Position ( $y/H$ )	0.25	0.50	1.00	1.50	2.25
Condition A	140.67	57.94	29.10	16.21	8.61
Condition B	55.71	26.83	12.42	7.43	3.91
Condition C	---	13.80	6.75	4.18	2.41
Condition D	---	---	4.30	---	1.71
Condition B (h)	---	27.32	---	---	4.04
Condition D (h)	---	---	4.57	---	---

It is interesting to observe the similar behavior in the different conditions regarding the configuration of vertical profiles of mean concentration. Regarding the concentration fluctuations, the  $I_c$  intensity profiles also show a similar behavior under the different conditions with the exception of the D condition. The general behavior indicates a configuration with smooth variations with a peak of the fluctuations in the position just above the point defining the maximum value in the mean concentration profile.

The horizontal profiles of mean concentration show a Gaussian and symmetrical configuration, due to the absence of a lateral limitation. In the case of fluctuation intensities, the profiles define two peaks, approximately at points located at a distance  $x/H = 0.1$  to the left and right of the point corresponding to the maximum value in the mean concentration profile.

## RESULTS FOR EMISSION DOWNWARD SIMULATING THE ROCKET – MODEL $0^\circ$

The results obtained in the rocket simulation are shown. The survey was performed considering the incident wind direction corresponding to  $0^\circ$ . Table 3 shows the characteristics that define the plume dispersion conditions for emission from top to bottom (E, F, G, H and I).

**Table 3.** Conditions for emission downward.

Condition	$Q_0$ [ $\text{dm}^3/\text{s}$ ]	$w_0$ [ $\text{m/s}$ ]	$U_{ref}$ [ $\text{m/s}$ ]	$w_0/U_{ref}$
E	0.176	2.241	2.60	0.862
F	0.703	8.951	2.60	3.443
G	1.582	2.143	2.60	7.747
H	0.176	2.241	1.65	1.358
I	0.703	8.951	4.55	1.967

Figure 14 shows the vertical profiles of the non-dimensional mean concentration  $K$  and the intensity values of the concentration fluctuations  $I_c$  obtained in the leeward positions of the emission, with spacings and  $/H$  of 0.25, 0.75 and 2.25 respectively. The helium flow rate was  $0.176 \text{ dm}^3/\text{s}$  and the reference air velocity is  $2.60 \text{ m/s}$ , which defines condition E for the emission.

Figure 15 shows the vertical profiles of concentration  $K$  and intensity  $I_c$  obtained with an emission of helium of  $0.703 \text{ dm}^3/\text{s}$  that determines the condition F for the emission. The leeward positions of the emission are  $y/H$  of 0.25, 0.50, 0.75, 1.50 and 2.25, respectively.

The profiles corresponding to condition G, obtained with a helium flow of  $1,582 \text{ dm}^3/\text{s}$  and air velocity of  $2.60 \text{ m/s}$ , are shown in Fig. 16. The positions presented are  $y/H = 0.50, 0.75$  and  $2.25$ , respectively. The condition H, defined from an emission of  $0.176 \text{ dm}^3/\text{s}$  of helium and an air reference velocity of  $1.65 \text{ m/s}$ , is presented in Fig. 17 for the position  $y/H = 2.25$ . In this same figure, condition I, corresponding to the emission of  $0.703 \text{ dm}^3/\text{s}$  of helium and an air reference velocity of  $4.55 \text{ m/s}$ , is presented for the position  $y/H = 0.25$ .

Figure 18 shows two horizontal profiles corresponding to the F condition of the emission plume obtained in the leeward positions of the emission  $y/H = 0.25$  and  $0.75$  to evaluate the lateral symmetry of the emission plume.

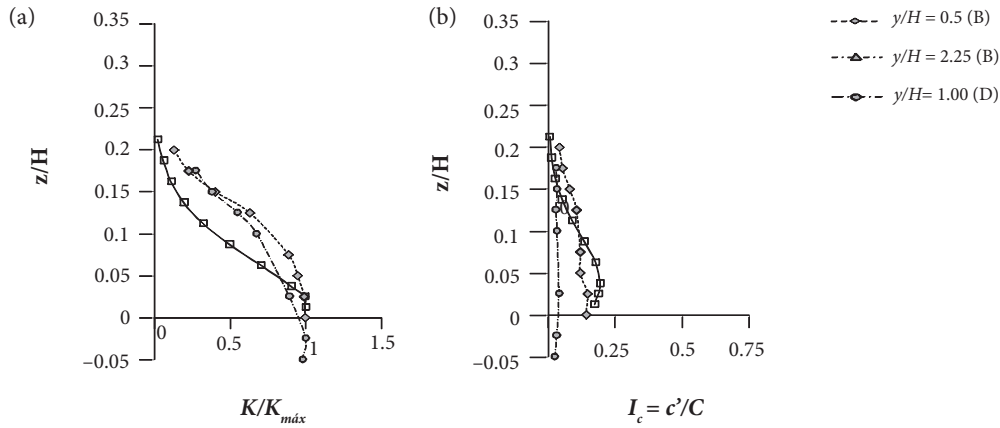


Figure 14. Vertical profiles of concentration (a)  $K/K_{max}$ ; and (b)  $I_c$  for condition E.

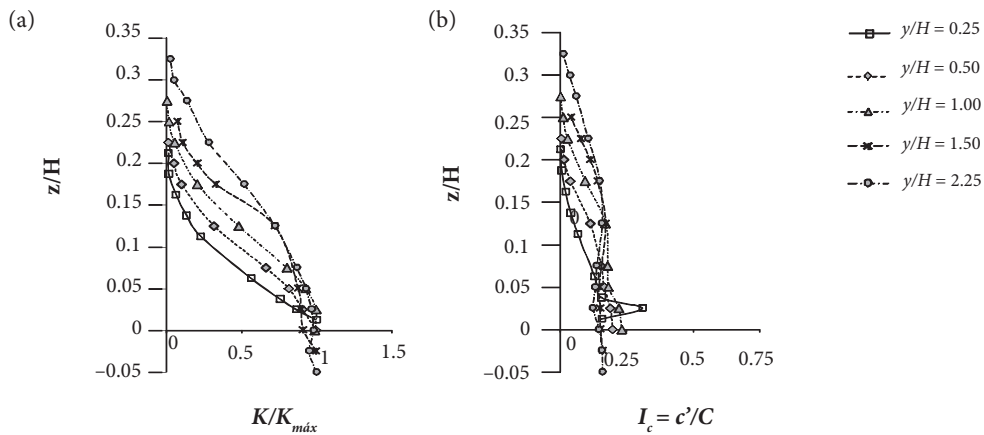


Figure 15. Vertical profiles of concentration (a)  $K/K_{max}$ ; and (b)  $I_c$  for condition F.

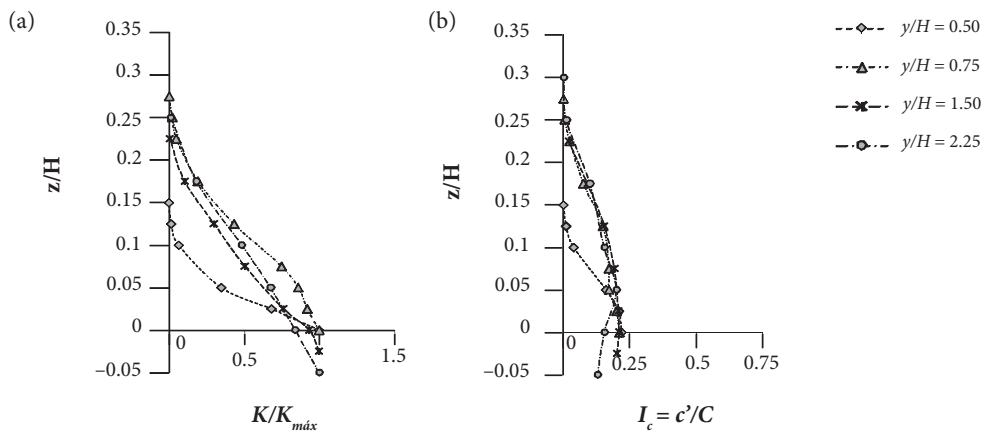
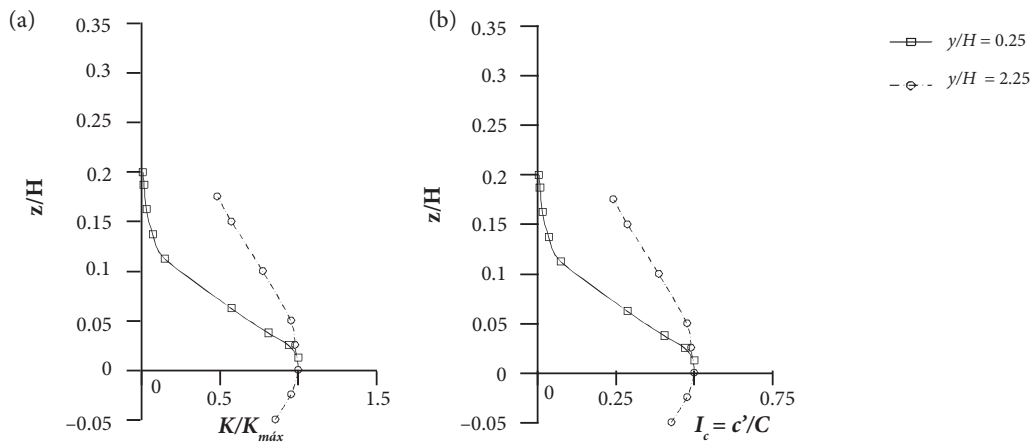
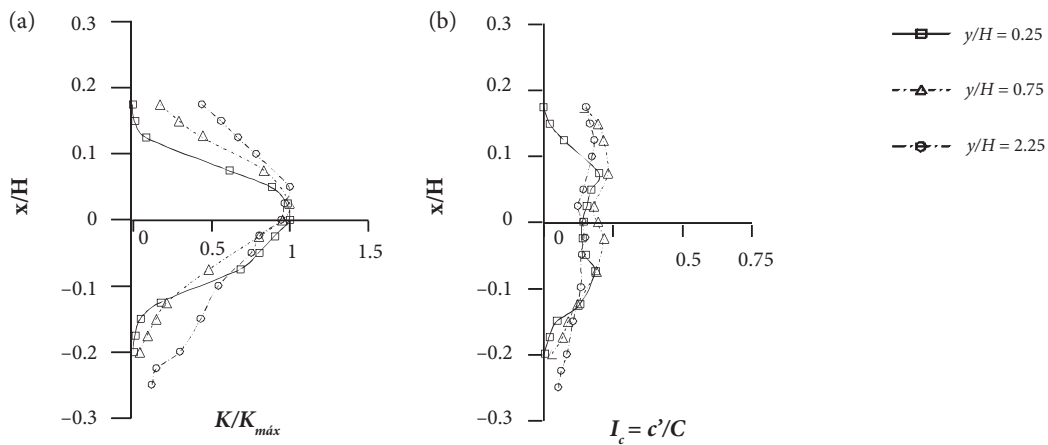


Figure 16. Vertical profiles of concentration (a)  $K/K_{max}$ ; and (b)  $I_c$  for condition G.





**Figure 17.** Vertical profiles of concentration (a)  $K/K_{m\acute{a}x}$ ; and (b)  $I_c$  for conditions H and I.



**Figure 18.** Horizontal profiles of concentration (a)  $K/K_{m\acute{a}x}$ ; and (b)  $I_c$  for condition F.

Also in this case, the results are complemented with the values of  $K_{m\acute{a}x}$  (Table 4) that allow evaluating the evolution of the dispersion process in terms of the position of the profile. Likewise, the results show consistency with respect to the analysed conditions, and to the distribution of the measured values in the different positions.

**Table 4.** Values of  $K_{m\acute{a}x}$  for emission downward – model O°.

Position ( $y/H$ )	0.25	0.50	0.75	1.00	1.50	2.25
Condition E	69.78	---	16.19	---	---	7.32
Condition F	51.68	24.51	---	16.68	8.45	5.34
Condition G	---	9.86	7.99	---	3.11	2.96
Condition H	---	---	---	---	---	5.05
Condition I	110.15	---	---	---	---	---
Condition F (h)	52.71	---	18.22	---	---	5.42

Regarding the configuration of vertical profiles of medium concentration, the different conditions show greater differences than in the previous case. The  $I_c$  concentration intensity profiles also do not show a similar behavior under the different conditions.

The general behavior indicates a configuration with smooth variations, but without the clear definition of a peak as it happens in the case of emission at ground level.

The horizontal profiles of mean concentration also do not show a Gaussian symmetrical configuration as in the case of emission at the ground level. In the same way, the profiles of the fluctuation intensities  $I_c$  show two peaks, but they are not well defined as it happens in the previous case.

**RESULTS FOR EMISSION DOWNWARD SIMULATING THE ROCKET – MODEL 330°**

Some results were obtained in the direction corresponding to the incident wind direction at 330°. The vertical profiles of concentration  $K$  and the intensity of the fluctuations  $I_c$  obtained at the  $y/H$  positions of 0.25, 0.75 and 1.50, respectively, for the emission condition F, are shown in Fig. 19. Table 5 indicates the values of  $K_{m\acute{a}x}$  to evaluate the evolution of the concentration profiles.

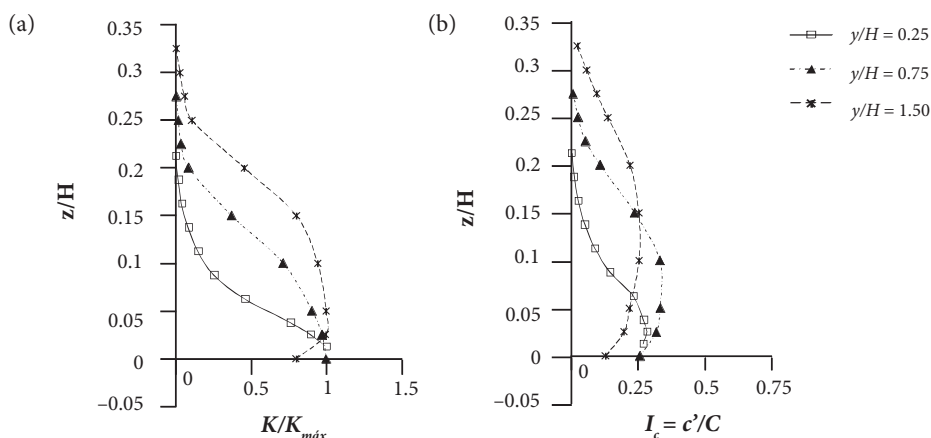


**Figure 19.** Vertical profiles of concentration (a)  $K/K_{m\acute{a}x}$ ; and (b)  $I_c$  for condition F.

**Table 5.** Values of  $K_{m\acute{a}x}$  for emission downward – model 330°.

Position ( $y/H$ )	0.25	0.75	1.50
Condition F	58.11	19.42	10.02

**DISCUSSION OF RESULTS**

Results for emission at ground level presented in Figs. 9 to 13 indicate a Gaussian behavior of the concentration vertical profiles in the upper part of the plume. Some modifications of the profiles are produced in the lower part (close to the floor) with relation to Gaussian behavior. Table 2 indicates a gradual diminution of maximum concentration values from the nearest position of the emission to the far away position. Comparison of vertical profile configurations near the emission with respect to emitted gas volume indicates maximum concentration at ground level with minor emitted gas (condition A), while the maximum concentration in the case of maximum emission (condition C) occurs at  $z/H = 0.10$ .

Figures 14 to 18 for emission downward and model 0° show different behaviors according to the emission condition analysed. Differences with relation to Gaussian behavior are more evident in some cases. Results obtained for condition F show values more similar to the results obtained with ground level emission, however, the vertical dispersion is always greater for emission downward cases. At the same time, intensities of concentration fluctuations are always minor than 0.25 in these cases, while the corresponding values for ground level emission are clearly greater.

General comparison between the plume behaviour for incident wind direction of  $0^\circ$  (Fig. 15) and  $330^\circ$  (Fig. 19) indicates maximum values of concentration a little greater for direction  $0^\circ$ . The same occurs with respect to the values of the fluctuating concentration. This behavior is coherent with the topographic configuration related to each incident wind direction, being that the slope upwind the emission is greater for direction  $0^\circ$ . Previous measurements of atmospheric flow indicated turbulence levels leeward emission greater for the case of wind direction of  $330^\circ$ . So, the mixing process is faster and the dispersion is greater diminishing the concentration fluctuations.

---

## CONCLUSIONS

The work presents the experimental evaluation of the dispersion process at the ALC region. A quantitative analysis of the vertical and horizontal profiles of the mean concentration and fluctuation intensity, and comparisons between results obtained for two incident wind directions were carried out by tests using wind tunnel.

The general comparison between the values obtained for the emission at ground level and for the case of the emission downward indicates greater concentration dilution for the first case. These results are predictable taking into account that the turbulent diffusion can be developed upward, downward and laterally in the case of the ground level emission.

The importance of the incident wind simulation and topographical model are shown in this paper. The use of wind tunnel tests to analyse this type of phenomena is also highlighted.

In general, results obtained with the emission at ground level indicate a similar behavior with previous work (Wittwer *et al.* 2007b; 2011), and the evolution of the  $K_{max}$  values are coherent with dilution factor obtained for this type of process (Chui and Wilson 1988; Saathoff *et al.* 1998). Similar experimental studies considering the case of the emission downward are not found in the specific literature, but the obtained general behavior and the measured values showed coherence with respect to the case of the emission at ground level. A multilayer model to simulate rocket exhaust clouds was developed by Moreira *et al.* (2011) and further simulations to analyse dispersion process using this model will permit to complete this experimental study.

---

## AUTHOR'S CONTRIBUTION

Conceptualization, Wittwer A, Loredo-Souza A and Oliveira M; Methodology, Wittwer A, Loredo-Souza A and Oliveira M; Investigation, Wittwer A, Loredo-Souza A, Oliveira M, and Souza B; Writing – Original Draft, Wittwer A, Loredo-Souza A, Oliveira M, Fisch G and Goulart E; Writing – Review and Editing, Souza B.

---

## REFERENCES

- Blessmann J (1982) The boundary layer tv-2 wind tunnel of UFRGS. *Journal of Wind Engineering and Industrial Aerodynamics* 10(2):231-248. doi: 10.1016/0167-6105(82)90066-6
- Blessmann J (1995) *O vento na engenharia estrutural*. Porto Alegre: Editora da Universidade, UFRGS.
- Cao S, Tamura T (2006) Experimental study on roughness effects on turbulent boundary layer flow over a two-dimensional steep hill. *Journal of Wind Engineering and Industrial Aerodynamics* 94(1):1-19. doi: 10.1016/j.jweia.2005.10.001
- Chui EH, Wilson DJ (1988) Effect of varying wind direction on exhaust gas dilution. *Journal of Wind Engineering and Industrial Aerodynamics* 31(1):87-104. doi: 10.1016/0167-6105(88)90189-4
- Counihan J (1969) An improved method of simulating an atmospheric boundary layer in a wind tunnel. *Atmospheric Environment* 3(2):197-214. doi: 10.1016/0004-6981(69)90008-0
- Degrazia GA, Anfossi D, Carvalho JC, Mangia C, Tirabassi T, Campos Velho HF (2000) Turbulence parameterisation for PBL dispersion models in all stability conditions. *Atmospheric Environment* 34(21):3575-3583. doi: 10.1016/S1352-2310(00)00116-3

- Delaunay D, Lakehal D, Barré C, Sacré C (1997) Numerical and wind tunnel simulation of gas dispersion around a rectangular building. *Journal of Wind Engineering and Industrial Aerodynamics* 67-68:721-732. doi: 10.1016/S0167-6105(97)00113-X
- Faria AF (2016) Análise experimental do escoamento atmosférico no Centro de Lançamento de Alcântara utilizando túnel de vento (Master's Dissertation). São José dos Campos: Instituto Tecnológico de Aeronáutica. In Portuguese.
- Fisch G (2010) Comparisons between aerovane and sonic anemometer wind measurements at Alcântara Launch Center. *Journal of Aerospace Technology and Management* 2(1):105-110. doi: 10.5028/jatm.2010.0201105110
- Gisler CAF, Fisch G, Correa CDS (2011) Análise estatística do perfil de vento na camada limite superficial no Centro de Lançamento de Alcântara. *Journal of Aerospace Technology and Management* 3(2):193-202. doi: http://10.5028/JATM.2011.03022411
- Harion J, Camano E, Favre-Marinet M (1995) Mesures de vitesse et de concentration par thermo-anémométrie dans des mélanges air/hélium. *C R Acad Sci Paris* 320(2):77-84.
- Jensen NO, Busch NE (1982) *Atmospheric Turbulence*. Amsterdam: Elsevier.
- Kastner-Klein P, Plate EJ (1999) Wind-tunnel study of concentration fields in street canyons. *Atmospheric Environment* 33(24-25):3973-3979. doi: 10.1016/S1352-2310(99)00139-9
- Loredo-Souza AM, Schettini EBC, Paluch MJ (2004) Simulação da camada limite atmosférica em túnel de vento. Presented at: IV Escola da Primavera Transição e Turbulência. Anais da IV Escola da Primavera Transição e Turbulência; Porto Alegre, Brazil.
- Loredo-Souza AM, Wittwer AR (2010) Estudo em Túnel de Vento do Processo de Dispersão de Gases no Centro de Lançamento de Alcântara. Technical Report. Laboratório de Aerodinâmica das Construções.
- Magnago R, Fisch G, Moraes O (2008) Análise Espectral do Vento no Centro de Lançamento de Alcântara (CLA). *Revista Brasileira de Meteorologia* 25(2):19.
- Marinho Pires LB, Roballo S, Fisch G, Avelar A, Girardi R, Gielow R (2010) Atmospheric flow measurements using the PIV and HWA techniques. *Journal of Aerospace Technology and Management* 2(2):127-136. doi: 10.5028/jatm.2010.02027410
- Marvoldis I, Griffiths JS, Hall DJ (2003) Field and wind tunnel investigations of plume dispersion around single surface obstacles. *Atmospheric Environment* 37(21): 2903-2918. doi: 10.1016/S1352-2310(03)00300-5
- Meroney RN, Leitl BM, Rafailidis S, Schatzmann M (1999) Wind-tunnel and numerical modeling of and dispersion about several building shapes. *Journal of Wind Engineering and Industrial Aerodynamics* 81(1-3):333-345. doi: 10.1016/S0167-6105(99)00028-8
- Moreira DM, Trindade LB, Fisch G, Moraes MR, Dorado RM, Guedes RL (2011) A multilayer model to simulate rocket exhaust clouds. *Journal of Aerospace Technology and Management* 3(1):41-52. doi: 10.5028/jatm.2011.03010311
- Novak MD, Wardland JS, Orchansky AL, Ketler R, Green S (2000) Wind tunnel and field measurements of turbulence flow in forests. Part I: uniformly thinned stands. *Boundary Layer Meteorology* 95(3):457-495. doi: 10.1023/A:1002693625637
- Pires LBM, Fisch G, Gielow R, Souza LF, Avelar AC, Paula IB, Girardi R (2015) A study of the internal boundary layer generated at the Alcântara Space Center. *American Journal of Environmental Engineering* 5(1A):52-64. doi: 10.5923/s.ajee.201501.08
- Roballo ST, Fisch G (2008) Escoamento atmosférico no Centro de Lançamento de Alcântara (CLA): Parte I - aspectos observacionais. *Revista Brasileira de Meteorologia* 23(4):510-519.
- Saathoff P, Stathopoulos T, Wu H (1998) The influence of the freestream turbulence in nearfield dilution of exhaust from building vents. *Journal of Wind Engineering and Industrial Aerodynamics* 77-78:741-752. doi: 10.1016/S0167-6105(98)00188-3
- Schuch D, Fisch G (2017) The use of an atmospheric model to simulate the rocket exhaust effluents transport and dispersion for the Centro de Lançamento de Alcântara. *Journal of Aerospace Technology and Management* 9(2):137-146. doi: 10.5028/jatm.v9i2.740
- Standen NM (1972) A Spire Array for Generating Thick Turbulence Shear Layers for Natural Wind Simulation in Wind Tunnels. (LTR-LA-94). NAE Technical Report.
- Surry D (1982) Consequences of distortions in the flow including mismatching scales and intensities of turbulence. Presented at: International Workshop on Wind Tunnel Modeling Criteria and Techniques in Civil Engineering; Gaithersburg, USA.
- Wittwer AR (2006) Simulação do vento atmosférico edos processos de dispersão de poluentes em túnel de vento (PhD Thesis). Porto Alegre: Universidade Federal do Rio Grande do Sul. In Portuguese.
- Wittwer AR, Loredo-Souza AM, Schettini EBC (2007a) Avaliação das flutuações de concentração em uma pluma de dispersão de poluentes. *Ciência e Natura Edição especial*:141-144.
- Wittwer AR, Paoli F, Loredo-Souza AM, Schettini EBC (2007b) Wind tunnel study of the concentration fields in a plume emission. Presented at: International Workshop on Physical Modelling of Flow and Dispersion Phenomena; Orléans, France.



Wittwer AR, Loredou-Souza AM, Schettini EBC (2011) Laboratory evaluation of the urban effects on the dispersion process using a small-scale model. Presented at: 13th International Conference on Wind Engineering. Proceedings of the ICWE13; Amsterdam, The Netherlands.

Wittwer AR, Loredou-Souza AM, Oliveira MGK, Souza BH, Fisch G, Goulart EV (2016a) Estudo do processo de dispersão turbulenta de gases no Centro de Lançamento de Alcântara. Presented at: 10th ABCM Spring School on Transition and Turbulence; São José dos Campos, Brazil.

Wittwer AR, Loredou-Souza AM, Oliveira MGK, Souza BH, Fisch G, Goulart EV, Carvalho GF (2016b) Simulação das características do vento atmosférico no Centro de Lançamento de Alcântara. Presented at: 10th ABCM Spring School on Transition and Turbulence; São José dos Campos, Brazil.

Zanetti P (1990) Air pollution modeling: theories, computational methods and available software. New York: Van Nostrand Reinhold.